Astron. Astrophys. 213, 339–350 (1989)

ASTRONOMY AND ASTROPHYSICS

The spatial relationship of OH and H_2O masers

J.R. Forster[1,2] **and J.L. Caswell**[2,3]

[1] Division of Radiophysics, CSIRO, Australia Telescope, Paul Wild Observatory, PO Box 94, Narrabri, NSW 2390, Australia
[2] Division of Radiophysics, CSIRO, PO Box 76, Epping, NSW 2121, Australia
[3] Dominion Radio Astrophysical Observatory, Herzberg Institute of Astrophysics, National Research Council of Canada, Penticton, B.C., Canada V2A 6K3

Received June 22, accepted October 10, 1988

Summary. Results of VLA observations of OH and H_2O masers associated with 74 star-forming regions are presented. Absolute positions of reference features for both molecular species are given to an accuracy of 0.5″ rms. This sample greatly increases the statistics for studying the spatial relationship between OH and H_2O masers, and compact H II regions.

The OH and H_2O maser groups in associations generally overlap, or are separated by less than a few arcsec. The majority of OH/H_2O associations are simple, consisting of one OH and one H_2O group, both groups typically <30 mpc ($\sim 10^{17}$ cm, ~ 6000 AU) in diameter. A number of associations are complex, containing multiple maser groups and often compact continuum emission. In these cases the OH and H_2O groups are intermixed, but not coincident, and are spread over a region typically 150 mpc in extent. The spatial extent of OH maser emission in these complexes is correlated with the velocity spread.

The close association of the two maser species, combined with a lack of detailed correlation, suggests that the OH and H_2O masers occur near a common energy source but in physically distinct zones. The size and complexity of a maser cluster may indicate the evolutionary stage of its associated star.

Key words: star formation – masers –H II regions

1. Introduction

Various ideas concerning the formation of OH masers associated with star-forming regions have been proposed since their discovery in the 1960s (Weaver et al., 1965). Cook (1968) proposed that OH masers form in the compressed zone just outside an expanding H II region, while Mezger and Robinson (1968) suggested that OH masers delineate individual protostars triggered into collapse by the expansion. Several authors (e.g. Norris, 1984; Heaton et al., 1985; Brebner et al., 1987) have suggested that OH masers are contained in disks surrounding massive young stars. Baart and Cohen (1985) argue that OH masers lie in the expanding molecular envelope outside an ionization front, in agreement with the model of Elitzur and de Jong (1978). This represents a return to the original suggestion of Cook, aspects of which are present in most models for OH maser excitation. The presence of a massive star capable of producing an H II region is common to all of these models. Although H II regions are not detected at the position of all OH masers, this could be due to the small size of very young H II regions and sensitivity limitations. For example, an optically thick H II region of size 0.2″ (~ 5 mpc at a distance of 5 kpc) and temperature 10^4 K has a 22 GHz flux density of ~ 150 mJy.

Ideas concerning the formation and excitation of H_2O masers also abound. Baudry et al. (1974) suggested that the H_2O masers in W49 are pumped collisionally, and are associated with objects which are not gravitationally bound. Accurate position measurements (Hills et al., 1972; Forster et al., 1978) showed that some H_2O masers occur in small groups just beyond the boundaries of continuum sources. This led to the suggestion that H_2O masers arise in molecular fragments excited by collisions with an expanding H II region. A contrasting view arose on the basis of VLBI data, with Genzel et al. (1978) concluding that individual H_2O maser groups are each excited by an embedded star. However, proper motion studies of H_2O masers in Orion (Genzel et al., 1981) showed that some H_2O masers are involved in high-velocity outflow from a central source; this showed that not all masers are confined to circumstellar envelopes, and led to renewed interest in collisional models (Norman and Silk, 1979; Deguchi, 1981; Tarter and Welch, 1986).

Nonetheless, it is still not certain whether compact maser groups generally represent individual stars in a dense star-forming region, or molecular fragments spread over the region of influence of a single exciting source.

Despite the many years that have elapsed since the discovery of H_2O masers (Cheung et al., 1969), the positions of both OH and H_2O masers in associations have been accurately measured for only a handful of sources. Hills et al. (1972) noted significant separations between the OH and H_2O masers in Orion and W3(OH), and suggested that the two molecular species might form under different conditions. Large separations were also found for OH and H_2O masers in W49 and W51 (Mader et al., 1978) using VLBI techniques. These and other studies suggest that OH and H_2O masers may not be closely related.

On the other hand, regions containing OH masers appear to be the best sites for detecting H_2O maser emission, and a close association is implied by many models of maser excitation. If both maser species are found in the molecular envelopes of young stars (e.g. Genzel and Downes, 1977) then OH and H_2O masers should coincide closely, as in evolved stars. If H_2O masers reside in

Send offprint requests to: J.R. Forster

molecular fragments near H II regions (e.g. Forster et al., 1978), the two species should be closely associated if not coincident. In order to account for pairs of OH and H_2O maser groups which lie close together but with small yet definite offsets, Caswell et al. (1983a) postulated the development of binary fragments in star formation, one containing OH masers and the other containing H_2O.

In order to clarify the situation we have observed ~70 regions containing masers of both molecular species with the Very Large Array (VLA). These associations (taken from Caswell et al., 1983a, b) form a substantially complete and unbiased sample of OH and H_2O masers with angular separation $<15''$ in the galactic longitude range 339° to 50° (observable from both the northern and southern hemispheres). The positional accuracy obtained with the VLA is sufficient to establish coincidence of the two species to within ~1″ rms, equivalent to 25 mpc (1 mpc $=3.1\ 10^{15}$ cm ~200 AU) at a distance of 5 kpc. This is the first study in which a statistically meaningful sample of associated OH and H_2O masers has been observed with similar resolution at both frequencies, and with good relative positional accuracy.

In this paper we give absolute positions of OH and H_2O masers to an estimated accuracy of ~0.5″ rms. We then discuss both the extent and displacement of OH and H_2O maser emission, and the spatial relationship of the masers and compact H II regions for the sample as a whole. The detailed maser distributions and kinematics of individual sources will be discussed in a later paper.

2. Observations and data reduction

The 1665 MHz OH observations were carried out in December 1983 using the VLA[1] in its A-B hybrid configuration with baselines up to 22 km. The 22, 235 MHz H_2O observations were made in June 1984 in C configuration, using baselines up to 2.6 km. Each observation consisted of an 8-min snapshot followed by a 3-min calibration. The sense of circular polarization used for the OH sources was based on previous observations with the Parkes telescope (Caswell and Haynes, 1983a, b). All of the H_2O observations were made in right circular polarization.

The correlator was configured to provide 64 frequency channels covering bandwidths of 0.195 and 6.25 MHz for the OH and H_2O observations respectively. With this number of channels only 18 of the 27 antennas could be used. The corresponding velocity resolutions were 0.55 and 1.32 km s^{-1} after Hanning smoothing. The rms noise in a naturally weighted single channel map was ~0.1 Jy for both sets of observations.

The same calibration sources were used for both the OH and H_2O observations. Amplitude calibration was based on the source 1741-038 for which a flux density of 1.7 Jy at 1.7 GHz and 3 Jy at 22 GHz was assumed. Calibration sources were also used to check for variations in amplitude and phase over the passband. No bandpass corrections were applied since the variations were small and cause channel-to-channel relative position errors $<0.1''$.

After calibration and editing, a map was made on the DEC-10 in order to check the structure of a strong channel in each field. If the map showed simple point-source structure it was used as the reference channel (Table 1), otherwise another channel was selected. In the case of the 22 GHz data, the reference channel was used as a phase calibrator (in the program ANTSOL). This has the effect of eliminating atmospheric and instrumental effects from the spectral line data, and gives maser source positions relative to the reference feature. This procedure substantially improved the calibration of the H_2O channel maps, and provided a dynamic range typically >100. With normal VLA calibration the OH maps were generally limited by noise rather than dynamic range.

The visibilities were then mapped in the VLA PIPELINE linked computers, yielding ~1600 maps of OH masers and ~2700 maps of H_2O masers. The OH and H_2O map sizes were generally 32″ and 51″ square respectively, although in some cases larger maps were required. The maps were then transferred to tape for analysis elsewhere.

The OH maps were analysed at the Dominion Radio Astrophysical Observatory using the MAD (Manipulation And Display) computing facility. The H_2O maps were analysed at the Division of Radiophysics using AIPS image-processing software. In most cases the channel maps were cleaned and then visually inspected for the presence of maser emission. Positions were measured for all maser spots showing significant emission, but only masers with a signal-to-noise ratio >10 are included in the relative position analysis (Sect. 3). Channel maps free of maser emission were averaged to form continuum maps.

Most OH masers show a high degree of circular polarization and our intensity scale refers to the flux density contained in the single sense of circular polarization observed (and is only half the total flux density in the case of unpolarized features). We estimate the amplitude uncertainty for the OH observations to be ~20%. Our H_2O and 22 GHz continuum intensities correspond to an unpolarized source. These intensities may be in error by as much as ~50% owing to amplitude calibration uncertainties.

The error in absolute position is dominated by tropospheric and ionospheric effects which cause systematic delay variations across the array. Owing to the low elevations of the sources in our sample these effects can be large and variable. In order to estimate the probable error we have compared our positions with published positions for seven OH masers and continuum sources (Garay et al., 1985; Gaume and Mutel, 1987). The maximum error measured is 2.2″ for the 22 GHz continuum sources, and 1.9″ for OH. Assuming that the largest error is ~3σ and that most of the error is ours, we estimate a standard error in *absolute* position of ~0.5″ for our observations.

The error in measuring *relative* positions of unblended maser spots within an observed field is dominated by noise. For a signal-to-noise ratio of 10 the rms position error is ~4% of the FWHM beamwidth. The synthesized beam was typically elongated by about a factor of three, the largest dimension being ~5″ at 1.7 GHz and ~3″ at 22 GHz. Thus the relative error for masers brighter than 1 Jy is $<0.2''$ for both OH and H_2O. Likewise, the positional accuracy of a continuum source relative to a strong H_2O maser is ~0.2″ for a signal-to-noise ratio of 10 in the continuum map.

3. Results

3.1. Absolute positions

The amplitude, velocity and position of a reference OH and H_2O maser is listed in Table 1 for each field observed. The reference

[1] The VLA is operated by Associated Universities, Inc. under contract with the National Science Foundation.

Table 1. Positions of OH and H_2O reference features

Source (l°, b°)	OH Amp. (Jy)	OH Vel.[a] (km s^{-1})	OH Pol.[b]	OH RA (1950) h m s	OH Dec (1950) ° ' "	H_2O Amp. (Jy)	H_2O Vel.[a] (km s^{-1})	H_2O RA (1950) h m s	H_2O Dec (1950) ° ' "	HII Flux[c] (mJy)	Type[d]	Adopted distance (kpc)	Min. Sepn.[e] (arcsec)	Notes[f]
339.68-1.21	Not observed					5.0	-31.3	16 47 26.00	-46 11 02.4	<70		2.4		
339.88-1.26	16.2	-29.0	R	16 48 24.59	-46 03 29.0	1.3	-35.3	16 48 24.60	-46 03 34.7		(I)	3.1	4.8	
340.06-0.24	10.2	-53.8	R	16 44 35.92	-45 16 25.5	3.3	-51.0	16 44 35.93	-45 16 23.3	<80	S	4.6	2.2	
341.22-0.21	4.5	-37.6	R	16 48 41.57	-44 21 52.1	89.0	-39.6	16 48 41.65	-44 21 53.9	140	S	15.3	1.7	
343.13-0.06	72.0	-31.8	L	16 54 43.82	-42 47 34.7	59.0	-27.4	16 54 44.03	-42 47 36.6	<80	C	3.2	0.4	
344.23-0.57	1.0	-30.9	R	17 00 35.15	-42 14 29.7	Not Observed						3.4		
344.58-0.02	15.0	-2.3	R	16 59 26.48	-41 37 39.6	25.9	-4.0	16 59 26.43	-41 37 36.8	<60	S	0.7	2.2	
345.00-0.22	2.8	-25.3	R	17 01 40.26	-41 25 00.6	16.0	-24.0	17 01 40.14	-41 24 58.5	210	C	3.2	2.4	
345.01+1.79	15.7	-22.9	L	16 53 19.56	-40 09 46.4	14.8	-17.6	16 53 17.28	-40 09 23.2	310	(I)	3.0	6.4	1
345.41-0.95	1.0	-17.8	L	17 06 03.94	-41 32 09.3	16.4	-24.0	17 06 02.18	-41 32 06.3	530	(I)	2.3	20.0	
345.51+0.35	8.7	-19.6	R	17 00 53.43	-40 40 14.3	17.7	-26.9	17 00 53.55	-40 40 18.5	<20	(I)	2.1	3.8	
345.70-0.09	7.2	-6.0	L	17 03 20.78	-40 47 03.1	132.2	-6.0	17 03 21.03	-40 47 00.0	<160	(I)	(1.0)	3.5	
347.63+0.15	4.6	-94.4	L	17 08 24.22	-39 05 49.0	Not Detected					I	9.7		
348.55-0.98	2.3	-19.9	R	17 15 53.37	-39 00 49.9	Not Detected					I	2.5		
348.70-1.04	0.7	-11.6	R	17 16 37.15	-38 55 29.8	29.4	-13.4	17 16 39.83	-38 54 13.6	160	I	1.8	77.0	
348.89+0.10	2.4	-73.2	R	17 12 24.93	-38 06 52.7	Not Detected					I	8.9		
348.89-0.18	1.2	9.9	R	17 13 34.61	-38 16 12.3	1.2	6.3	17 13 34.67	-38 16 14.5		S	(1.0)	2.3	
349.07-0.02	2.3	14.9	R	17 13 25.60	-38 01 59.0	0.8	6.0	17 13 25.55	-38 01 58.8		S	(1.0)	0.6	
349.09+0.11	1.9	-81.5	L	17 12 59.77	-37 56 27.0	46.4	-80.0	17 12 59.62	-37 56 30.6	<70	(I)	9.8	3.4	1
350.02+0.43	1.1	-33.1	L	17 14 22.20	-37 00 02.5	3.0	-38.7	17 14 22.13	-37 00 03.2	110	(S)	5.0	1.1	
350.11+0.09	31.8	-71.1	R	17 16 02.14	-37 07 01.8	0.5	-62.1	17 16 01.18	-37 07 17.7		I	9.8	19.2	
351.16+0.70	35.7	-6.0	R	17 16 35.96	-35 54 50.6	16.2	-4.1	17 16 36.08	-35 54 51.0	<80	S	1.7	0.5	
351.42+0.64	8.6	-9.5	L	17 17 32.33	-35 44 02.1	69.3	-31.1	17 17 32.34	-35 44 02.5	2390	C	1.9	0.0	
351.58-0.35	7.8	-92.8	R	17 22 03.29	-36 10 05.7	33.4	-93.7	17 22 03.27	-36 10 05.5	1040	C	9.9	0.3	
351.78-0.54	81.0	-2.0	R	17 23 20.53	-36 06 45.3	78.3	12.1	17 23 20.32	-36 06 44.0	<160	C	2.2	0.8	
352.52-0.15	0.8	-48.6	R	17 23 50.75	-35 17 01.4	5.8	-46.3	17 23 50.87	-35 17 00.9	80	S	8.0	0.8	
353.41-0.36	1.3	-20.0	L	17 27 06.66	-34 39 29.5	31.2	-20.0	17 27 05.56	-34 39 21.7	520	(I)	4.5	15.7	1
353.46+0.56	1.0	-44.3	R	17 23 33.04	-34 05 53.6	0.7	-51.6	17 23 33.02	-34 05 54.6		S	8.4	1.0	
354.61+0.47	2.4	-15.7	R	17 26 59.99	-33 11 37.1	4.7	-9.8	17 26 59.99	-33 11 38.2	<30	S	4.2	1.1	
355.34+0.15	9.6	18.2	L	17 30 12.59	-32 45 55.7	7.4	9.7	17 30 12.54	-32 45 56.6	150	(I,S)	2.0	0.9	
358.23+0.11	2.8	-27.2	R	17 37 41.34	-30 21 07.5	28.0	-6.0	17 37 41.46	-30 21 08.6	<140	(S)	10.0	1.0	3
359.14+0.03	5.1	-1.7	R	17 40 13.99	-29 37 58.0	110.6	-1.0	17 40 13.96	-29 37 57.9	530	(S)	5.0	0.1	
359.44-0.10	4.6	-51.6	L	17 41 29.15	-29 27 02.8	7.3	-59.0	17 41 28.68	-29 26 59.8	<50	I	10.0	6.7	1
359.62-0.25	2.3	22.4	R	17 42 27.81	-29 22 20.2	5.3	20.6	17 42 27.70	-29 22 21.2	70	I,(S)	10.0	1.0	
359.97-0.46	13.0	14.5	L	17 44 09.17	-29 10 56.4	12.6	19.0	17 44 09.22	-29 10 57.7	<50	S	10.0	1.4	
0.38+0.04	2.2	35.4	R	17 43 11.27	-28 34 33.2	9.8	38.9	17 43 11.23	-28 34 34.0	<70	S	10.0	0.4	
0.55-0.85	2.3	19.2	R	17 47 03.91	-28 53 42.2	65.6	1.5	17 47 03.83	-28 53 39.5	<240	(S)	2.0	2.4	
2.14+0.01	2.8	59.4	R	17 47 28.21	-27 04 59.2	2.8	62.9	17 47 28.19	-27 04 59.2	<70	S	8.9	0.3	
3.91+0.00	4.1	17.7	R	17 51 33.02	-25 34 14.5	Not Detected					I	5.8		
5.88-0.39	5.4	13.7	L	17 57 26.71	-24 03 59.6	31.4	21.1	17 57 26.83	-24 03 56.5	6260	(I),C	2.6	0.4	
8.67-0.36	1.7	41.1	L	18 03 18.81	-21 37 52.6	6.8	31.0	18 03 18.75	-21 37 53.4	890	I,(S)	5.8	0.3	
9.62+0.20	7.9	1.2	R	18 03 15.86	-20 31 52.0	2.5	16.6	18 03 15.99	-20 31 54.9	<80	C	(2.0)	0.4	
10.62-0.38	6.7	-2.2	L	18 07 30.67	-19 56 28.4	51.5	0.0	18 07 30.56	-19 56 28.8	1920	C	6.0	1.2	
11.03+0.06	3.7	21.2	R	18 06 42.61	-19 21 57.0	0.8	12.4	18 06 42.56	-19 21 56.0	100	S	3.2	0.3	
11.90-0.14	6.6	40.5	L	18 09 15.19	-18 42 16.5	Not Detected					I	5.1		
12.22-0.12	0.8	26.8	R	18 09 48.45	-18 25 13.9	183.0	-0.5	18 09 43.81	-18 25 05.7	<150	I,S	16.1	0.9	
12.68-0.18	1.5	61.5	L	18 10 59.36	-18 02 39.6	242.2	58.7	18 10 59.17	-18 02 42.5	<60	I	6.4	3.6	
12.91-0.26	3.4	35.2	R	18 11 44.21	-17 52 58.0	7.7	37.7	18 11 44.18	-17 52 57.8	80	S	4.4	0.4	
14.17-0.06	Not Detected					36.6	47.6	18 13 32.25	-16 41 01.7	<80	I	5.0		
15.03-0.68	2.9	21.5	R	18 17 31.61	-16 12 57.8	6.9	16.7	18 17 29.91	-16 13 11.0	<120	I	2.5	3.4	1
16.59-0.05	2.2	58.9	L	18 18 18.16	-14 33 14.6	46.2	60.3	18 18 18.05	-14 33 14.7	<70	S	5.6	1.3	
19.61-0.13	1.0	53.0	R	18 24 29.05	-11 55 34.0	Not Detected					I	4.7		
19.61-0.23	4.1	41.5	R	18 24 50.24	-11 58 31.0	151.7	32.5	18 24 50.25	-11 58 31.7	360	C	3.8	0.2	
23.01-0.41	3.3	65.7	R	18 31 55.97	-09 03 02.7	9.0	79.0	18 31 56.10	-09 03 03.7	<70	I,S	12.8	1.1	
23.44-0.18	4.5	106.0	R	18 31 55.54	-08 34 04.7	73.4	101.3	18 31 55.53	-08 34 03.9	<90	I,S	7.8	0.1	
24.79+0.08	2.7	107.2	R	18 33 30.31	-07 14 42.5	81.7	110.3	18 33 30.43	-07 14 43.2	<300	I,S	7.7	0.7	
28.86+0.07	9.9	102.8	L	18 41 08.41	-03 38 34.5	61.3	106.3	18 41 08.28	-03 38 34.5	<80	S	8.5	1.3	
31.21-0.18	0.5	-29.5	L	18 46 21.05	-01 40 09.4	20.2	-37.9	18 46 20.91	-01 40 10.3	<140	S		2.4	3
31.24-0.11	3.5	21.1	L	18 46 09.51	-01 36 39.4	289.9	18.7	18 46 09.49	-01 36 38.8	310	(S)	1.6	0.7	
31.28+0.06	2.3	107.2	L	18 45 37.02	-01 29 53.8	5.2	109.0	18 45 36.44	-01 30 02.2	<70	I,(S)	8.5	2.0	
32.74-0.07	1.5	32.3	R	18 48 47.84	-00 15 42.8	70.0	32.4	18 48 47.81	-00 15 43.5	<80	S	2.5	0.3	
33.13-0.09	8.7	78.8	L	18 49 34.35	00 04 31.7	9.4	76.3	18 49 34.25	00 04 32.2	470	(I,S)	5.6	0.0	
34.26+0.15	18.9	56.0	L	18 50 46.33	01 11 14.6	368.4	60.3	18 50 46.36	01 11 13.9	4930	C	4.2	0.4	
35.03+0.35	7.5	47.2	R	18 51 29.16	01 57 30.6	18.5	68.5	18 51 29.12	01 57 30.7	<80	S	3.0	0.3	
35.20-0.74	5.1	36.6	R	18 55 41.04	01 36 31.2	19.9	22.1	18 55 41.05	01 36 31.1	<60	C	2.3	0.1	
35.20-1.74	0.6	32.1	L	18 59 13.16	01 09 11.8	15.5	46.6	18 59 13.24	01 09 13.5	1290	S	2.9	1.2	
35.58-0.03	20.2	48.9	R	18 53 51.37	02 16 29.4	9.9	50.0	18 53 51.38	02 16 29.4	190	(I,S)	3.5	0.1	
40.62-0.14	1.1	29.4	R	19 03 35.44	06 41 56.8	0.9	32.3	19 03 35.43	06 41 57.2		S	2.3	0.4	
43.80-0.13	41.0	41.1	L	19 09 30.97	09 30 46.4	575.0	41.3	19 09 30.98	09 30 46.8	310	(S)	11.8	0.1	
45.07+0.13	30.0	56.4	R	19 11 00.43	10 45 43.6	21.2	59.3	19 11 00.40	10 45 43.1	790	C	10.0	0.1	
45.47+0.13	7.1	59.0	L	19 11 46.15	11 07 02.8	4.4	62.6	19 11 45.97	11 07 02.9	<70	I	9.3	2.6	1
45.47+0.05	11.6	68.2	R	19 12 04.37	11 04 10.9	1.3	68.6	19 12 04.42	11 04 11.0		S	8.6	0.6	
48.61+0.02	3.5	19.5	L	19 18 13.00	13 49 45.8	80.8	38.5	19 18 12.93	13 49 44.7	<70	S	11.8	0.9	
49.49-0.39	38.2	58.6	R	19 21 26.30	14 24 36.9	394.0	84.4	19 21 26.32	14 24 41.8	2850	C,I	7.7	0.7	1,2

a) Velocities are with respect to LSR. b) Polarization is right (R) or left-hand (L) circular. c) HII flux density is the total at 22GHz.
d) Type: I = Isolated; S = Simple; C = Complex (see Section 4). Parentheses indicate classification uncertain.
e) Minimum separation of any OH and H_2O maser features.
f) Notes: 1) Contains multiple H_2O groups. 2) Contains multiple complex groups. 3) May be late-type star.

features were chosen on the basis of their intensity, but weaker features were preferred if the strongest ones were not compact; they are not necessarily the features of OH and H_2O with the smallest separations. We estimate a standard error of $\sim 0.5''$ for the positions listed, but note that errors of a few arcsec are suspected in some cases. The sense of circular polarization used for the 1665 MHz OH measurement and the continuum flux density measured at 22 GHz are also given. Where no continuum emission was detected at 22 GHz the noise level (3σ) of the continuum map is given as a crude upper limit. We assume that the 22 GHz continuum sources detected are H II regions since recombination lines have been observed from many of the stronger sources, and the 1.7 GHz measurements are in all cases compatible with a thermal spectrum.

3.2. Angular extent and separation of OH and H_2O masers

The OH and H_2O masers in a single channel map appear as one or more unresolved spots with the angular ($\sim 2''$) and velocity ($\sim 1\,km\,s^{-1}$) resolution of the VLA. Taking all channel maps together we find that the maser spots tend to occur in compact groups, sometimes with several separate groups appearing within the synthesized field of view. Most often H_2O groups outnumber OH groups in an association. The field 359.62−0.25 is shown as an example in Fig. 1. This field contains an isolated H_2O group, an OH/H_2O association (with the OH and H_2O groups separated by $\sim 1''$), and a compact H II region located ~ 200 mpc from the OH/H_2O association.

Histograms of the total angular extent of OH and H_2O maser emission for all fields in our sample are shown in Fig. 2a. The entire sample is shown shaded; darker shading distinguishes fields containing H II regions. The extent of OH emission is mainly confined to 5″, whereas many fields contain H_2O masers spread over much larger angles. In most cases this is due to the presence of two or more compact but well separated H_2O groups (e.g. Fig. 1). Omitting fields with H_2O extents $>15''$ and using 0.1″ binning, we find a median extent of 0.6″ for OH masers and 0.8″ for H_2O.

The peak in the distributions below 1″ is less pronounced for fields containing H II regions than for the sample as a whole. In other words, the OH and H_2O group extents tend to be larger when an H II region is present. This is not due to sensitivity limitations related to distance since the sources with detected continuum emission are not systematically nearer. Quantitatively, maser associations containing H II regions have median extents (after exclusion of fields with extent $>15''$) of 0.9″ for OH and 2.0″ for H_2O.

The distribution of angular separations between OH and H_2O masers is shown in Fig. 2b. The quantity histogrammed is the *minimum* separation between OH and H_2O masers; these separations are also listed in Table 1. The probable error associated with this measurement is the quadratic sum of the errors in absolute position for each species, or roughly $\sim 1''$ rms. Of the 59 associations with separations $<15''$, 61% have minimum separations $<1''$ and 88% are separated by $<2.5''$. The median

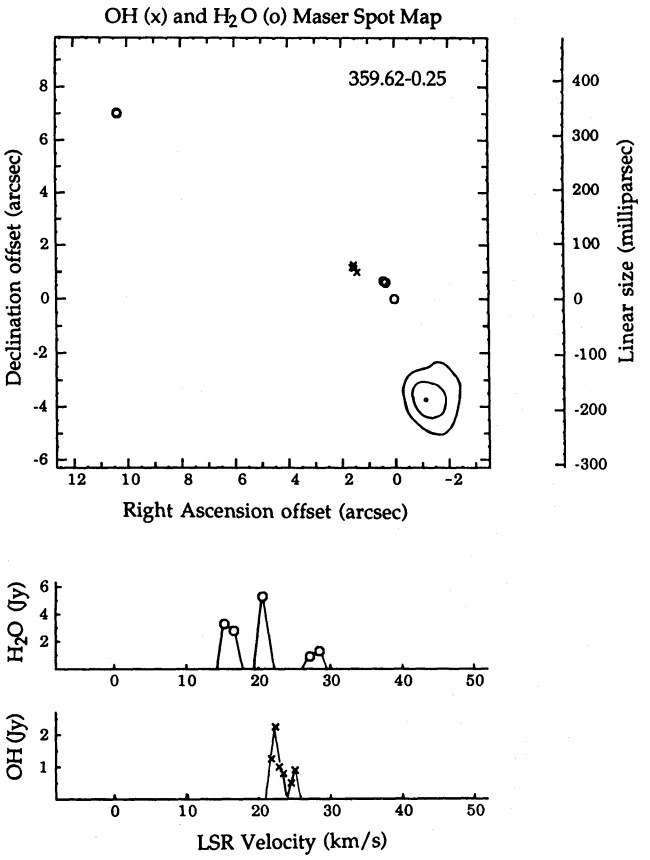

Fig. 1. OH (×), H_2O (○) and 22 GHz continuum contours (flux density levels are shown at 40 and 60 mJy/beam) for 359.62−0.25. The reference position is $17^h\,42^m\,27.70^s$, $-29°\,22'\,21.2''$. The VLA maser spectra are shown below the spot map

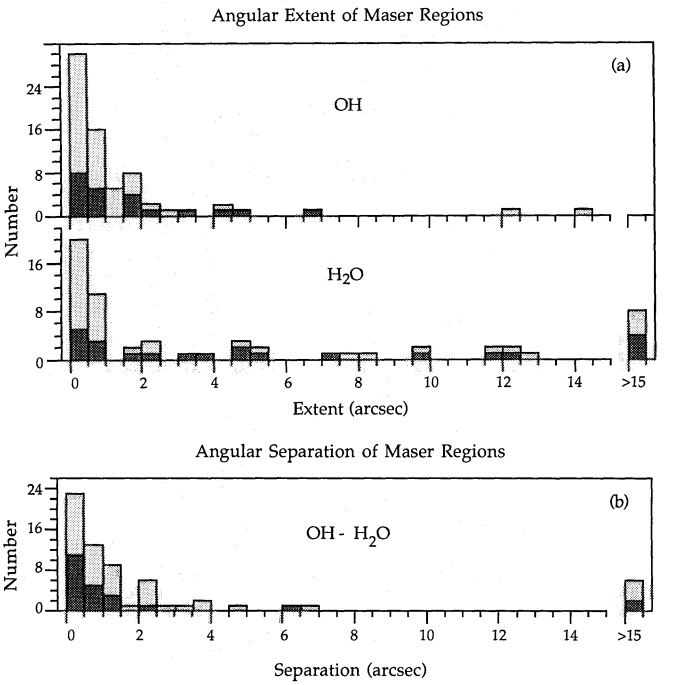

Fig. 2. a Histograms of the total angular extent of OH and H_2O emission for all fields mapped. Darker shading indicates fields in which compact continuum emission was detected. **b** Histogram of the minimum angular separation between OH and H_2O masers for all the fields surveyed

separation is 0.8″. For fields containing compact H II regions the minimum separation has a median value of 0.4″, indicating that the two maser species are generally intermixed in these cases.

3.3. *Linear extent and separation of OH and H_2O masers*

Linear sizes were derived from the measured angular extents using kinematic distances based on the OH maser velocities. A galactic centre distance of 10 kpc has been used in order to facilitate comparison with earlier publications. A preference for the near or far distance was based on additional information when available (mostly taken from Caswell et al. 1983a,b), otherwise the near distance was assumed. The adopted distances are listed in Table 1, with especially uncertain values enclosed in parentheses. The distribution of linear sizes is shown for both maser species in Fig. 3a. These are strictly projected linear sizes (i.e. lower limits) but will be referred to as linear sizes for brevity. Although appearing on a somewhat expanded scale, the distribution of linear sizes is qualitatively similar to that for angular sizes.

If we consider *group sizes* (i.e. omit large values of linear extent that mainly refer to *separations* of groups) we find that OH groups tend to be larger than H_2O groups. The median size for fields with linear extent <150 mpc is 15 mpc for OH and 9 mpc for H_2O. For masers near H II regions, the extent of OH and H_2O maser emission tends to be larger than for the sample as a whole.

The distribution of minimum linear separations between OH and H_2O masers is shown in Fig. 3b. This distribution is more strongly peaked near zero than the distribution of extents for either species, but it also contains a broad tail similar to the extent of H_2O emission. Of the 56 fields with OH–H_2O separations less than 150 mpc (i.e. "close" associations), 45% have separations <10 mpc and 46% have separations >20 mpc. Thus about half of these associations contain maser groups separated by less than the typical extent of individual maser groups (~ 15 mpc), and half have larger separations. The median separation for close associations is 12 mpc. The median separation for close associations containing H II regions is 7 mpc. Few associations containing H II regions have minimum separations >40 mpc.

3.4. *Separation of masers and H II regions*

For the 23 fields containing H II regions we show in Fig. 4 histograms of the minimum separation between the masers and the H II region. The separation is measured from the *peak* of the continuum emission to the *nearest* maser spot in each species. The estimated standard error in the angular displacement is $\sim 0.2''$ for H_2O and $\sim 1''$ for OH. In three fields (35.20−1.73, 19.61−0.23 and 49.49−0.39) we detect more than one H II region, and in these cases the strongest source is used for measuring separations. In only one case (19.61−0.23; see Fig. 8b) would a different choice reduce the minimum separation between the masers and H II region.

On an angular scale (Fig. 4a) the maser-H II region minimum separation has a similar distribution for both OH and H_2O masers. The median values for "close" ($<15''$ separation) associations are 1.1″ for OH and 0.7″ for H_2O. Given the uncertainty in the measurements, the difference in the two distributions is not significant. There is a tendency for H_2O masers not to coincide with the peak of the continuum emission: 60% of the peaks are separated from the nearest H_2O maser by more than 0.5″. For

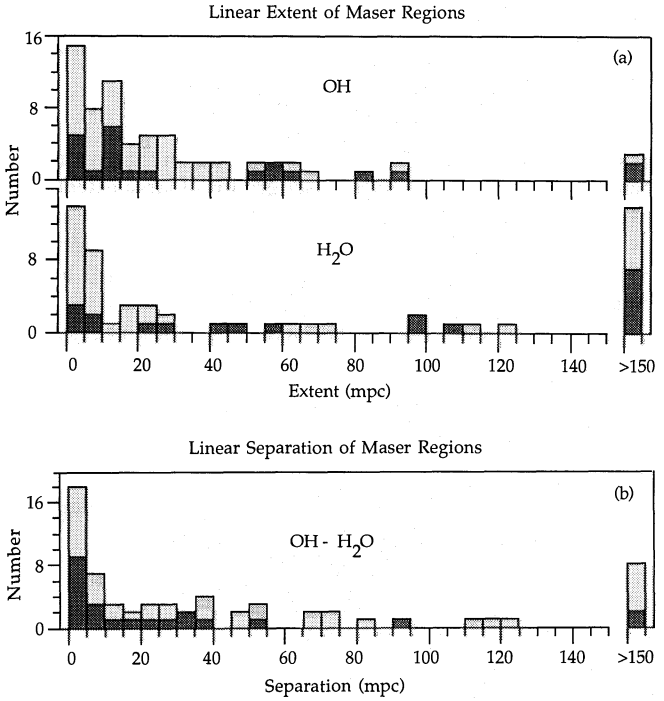

Fig. 3a and b. Same as Fig. 2, except the linear extent rather than the angular extent is shown. The units are in milliparsecs (1 mpc $=3.1\ 10^{15}$ cm)

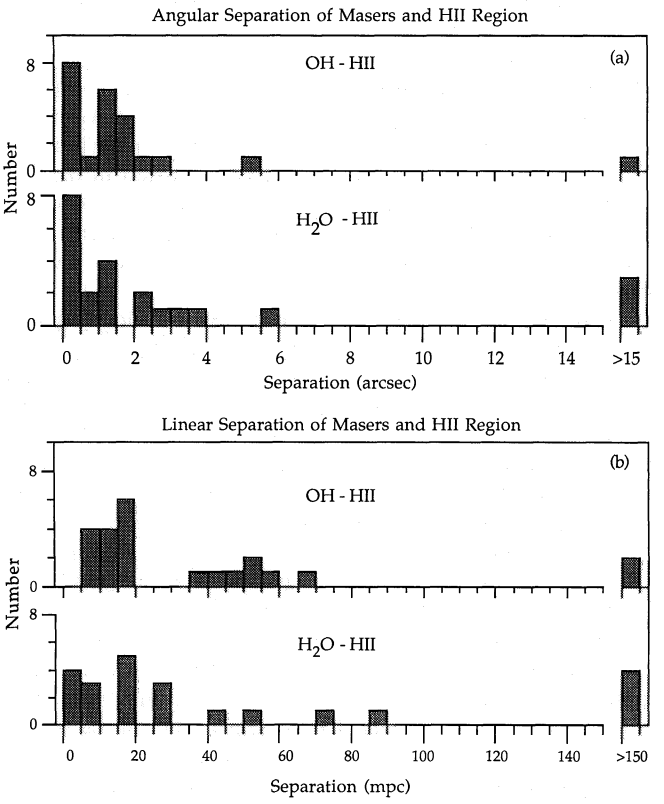

Fig. 4. a Histograms of the angular separation between the peak of the continuum emission and the nearest OH and H_2O maser for fields in which compact continuum emission was detected at 22 GHz. **b** Same as **a** except the linear separation is shown

OH masers the appearance is the same, although measurement errors weaken this conclusion. For the OH masers, 60% have minimum separations $>1''$. There is no clear evidence in our data that either species is located nearer to the peak of compact continuum emission. However, the *maximum* separation between the continuum peak and maser emission is generally greater for H_2O.

The distribution of minimum maser-H II separations on a linear scale is shown in Fig. 4b. The H_2O–H II distribution extends slightly farther than the OH–H II distribution, although both have median values of ~ 20 mpc. These distributions indicate that OH and H_2O masers are found close to, but not coincident with, the peaks of associated compact continuum sources. The typical separation of ~ 20 mpc is similar to the average size of maser groups, but is larger than the median separation between OH and H_2O groups associated with H II regions. In a typical OH/H_2O/H II association, OH and H_2O masers tend to occur close together and at a similar projected distance from the peak of the continuum emission. There may also be evidence for a bi-modal distribution of OH–H II separations, one involving a population with separations <20 mpc and another with separations between 35 and 60 mpc.

3.5. *Spatial and velocity correlations*

In order to see if a correlation exists between the spatial extents of OH and H_2O masers in close associations, we compare these in Fig. 5 for both angular (5a) and linear (5b) extents. Since absolute positions are not required for this comparison, the error is $\sim 0.2''$ in each coordinate, or about 5 mpc for a typical distance of 5 kpc. We define a good correlation as one in which at least 50% of the total variation in one quantity is accounted for by a linear relationship with the other quantity. This occurs if the sample correlation coefficient r exceeds 0.71 (cf. Freund 1971). A correlation coefficient of 0.39 is calculated for both scatter diagrams of Fig. 5, indicating that the extent of maser emission in the two species is not closely correlated. There is, however, a tendency for OH groups to be larger than H_2O groups; this can be seen from the predominance of points below the line of equal sizes in Figs. 5a and 5b.

Although scatter diagrams are not shown, the velocity spread of OH and H_2O masers in associations has been checked for correlation. A low coefficient ($r=0.16$) indicates that no significant correlation is present. Furthermore, no correlation ($r=0.05$) is found between the spatial separation of the strongest OH and H_2O masers in an association and their velocity difference. These results imply that the two maser species are not closely related kinematically, even though they occur in close associations.

In order to test for a correlation between the linear size and velocity extent of individual maser groups, these parameters are plotted in Fig. 6 for both OH and H_2O masers. No correlation is evident for H_2O masers (Fig. 6a). For the OH masers (Fig. 6b) the overall correlation coefficient is 0.42. However, the scatter diagram for OH masers is empty to the left of a line with slope ~ 10 mpc/km s^{-1}, suggesting that an upper limit on the spatial extent for a given velocity extent may exist. In addition, the size-velocity diagram for OH groups larger than ~ 30 mpc shows evidence for systematic behaviour. Applying the correlation test to the 13 OH groups with size >30 mpc and velocity spread <20 km s^{-1} we find $r=0.80$, indicating that a strong correlation is indeed present. The correlation coefficient for OH groups with

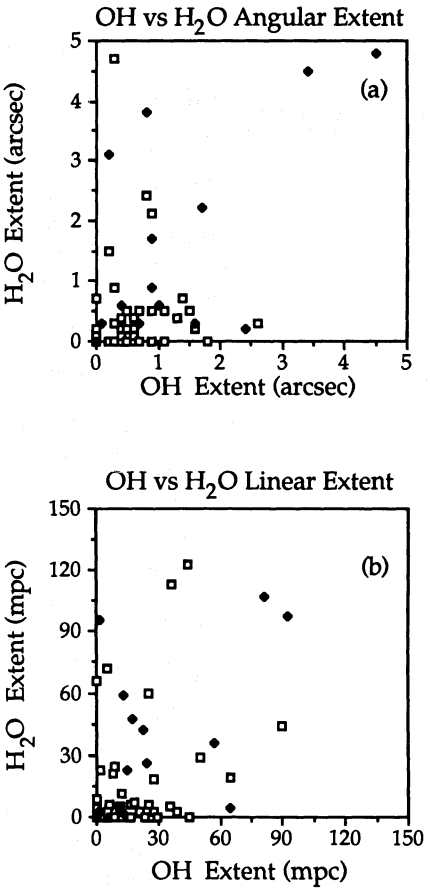

Fig. 5. a Scatter diagram of OH versus H_2O angular extent. Only fields in which the total extent of both species is $<5''$ are plotted. Fields without detected continuum emission are indicated by open squares; fields in which a compact H II region was detected are indicated by a filled diamond. **b** same as **a** except the linear extent of OH vs H_2O masers is plotted for fields with total extent <150 mpc

extent <30 mpc is 0.19, verifying the impression that systematic behaviour is restricted to OH maser groups of large extent. The two OH sources with extremely large velocity spread (~ 33 km s^{-1}) in Fig. 6b are 5.88–0.39 (with an H II region) and 351.78–0.54 (without). These two unusual sources will be discussed individually in a later paper.

Most of the sources with OH emission >30 mpc in extent are complex and contain multiple groups of both OH and H_2O masers. Six out of nine OH associations larger than 50 mpc contain detected H II regions. The more organized spatial-velocity behaviour of OH masers with large extent, along with the high incidence of H II regions in complex sources, suggests that the kinematics of large OH groups is related to the development of an H II region.

3.6. *Summary of results*

The median values obtained for the distributions discussed in this section are listed in Table 2. These values are based on "close" associations, i.e. associations with extents or separations less than $15''$ or 150 mpc. Median values are given (together with the number of fields included in the sample) for all fields, and

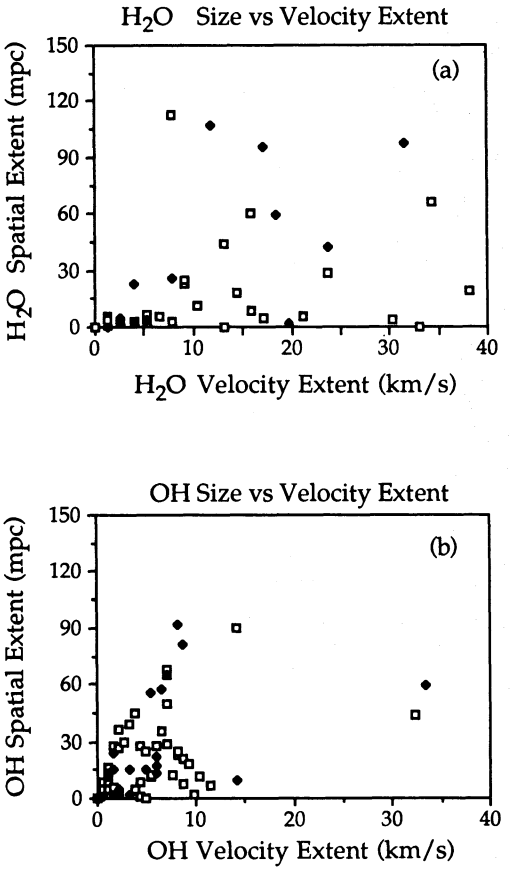

Fig. 6. a The linear extent is plotted against the velocity extent of H_2O maser emission. Fields containing detected H II regions are indicated by a filled diamond. Only fields with spatial extent <150 mpc and velocity extent $<40\ km\ s^{-1}$ are shown. **b** Same as **a** for OH masers

separately for the subset of fields in which compact H II regions were detected.

The main observational results can be summarized as follows:

1. OH masers tend to occur in groups of diameter 5 to 30 mpc.

2. H_2O masers tend to occur in more compact groups of size <10 mpc, and several groups may be present in a field.

3. H_2O groups outnumber OH groups by about 3 to 2 in our sample.

4. Simple associations containing essentially coincident, compact OH and H_2O groups comprise the majority of our sample.

5. A minority of associations are more complex, containing multiple OH and H_2O groups extending over ~ 150 mpc, and usually a nearby compact H II region.

6. In cases where a compact H II region is detected at 22 GHz, OH and H_2O masers are generally found within ~ 20 mpc of the peak of the continuum emission and typically extend to distances of ~ 65 mpc for OH and ~ 130 mpc for H_2O.

7. For most of the associations in our sample the OH and H_2O masers appear spatially intermixed. However, the detailed spatial and velocity distributions are not well correlated in the two species.

8. There is a correlation between the spatial extent and velocity spread for OH masers with extent >30 mpc. There is no such correlation apparent for H_2O masers.

4. Discussion

The 74 regions observed in this study represent a nearly complete sample of known OH/H_2O maser associations in the galactic longitude range 339° to 50°, a region covering more than half of the galactic disk. The sample undoubtedly comprises a range of evolutionary stages; it possibly includes different classes of masers but most of them are unambiguously associated with young star

Table 2. Median extents and separations

	All fields[a]		H II regions	
	Median	Number	Median	Number
Median values in **arcsec**				
OH extent	0.6	(69)	0.9	(22)
H_2O extent	0.8	(53)	2.0	(19)
OH–H_2O separation	0.8	(59)	0.4	(21)
OH–H II separation			1.1	(22)
H_2O–H II separation			0.7	(20)
Median values in **mpc**				
OH extent	15	(64)	15	(20)
H_2O extent	9	(44)	25	(13)
OH–H_2O separation	12	(56)	7	(21)
OH–H II separation			19	(21)
H_2O–H II separation			19	(19)

[a] Extents are not calculated for fields in which only one channel map contains significant maser emission (6 OH and 7 H_2O), and fields with extent $>15''$ (8 H_2O) are not included. Linear extents are not calculated for fields in which the kinematic distance is very uncertain (5 sources), and fields with total extent >150 mpc (3 OH and 16 H_2O) are not included.

forming regions (i.e. they do not exhibit strong 1612 MHz OH emission and lack the symmetrical velocity pattern typical of evolved stars). The intensity of 1665 MHz OH and 22 GHz H_2O maser emission makes these lines among the easiest to observe at radio wavelengths. However, the maser emission occurs in tiny spots often unresolved even by VLBI, and the various scale sizes of clumping makes the interpretation of spot maps difficult. The distribution of maser spots rarely gives a clear indication of the overall density structure in star-forming regions.

In our data a hierarchy of maser clustering is apparent which extends over scales from milliparsecs to parsecs. On the largest scale the clustering most probably corresponds to separate star-forming regions within a molecular cloud. On the smallest scales, association with an individual star is suggested. On intermediate scales (50–300 mpc) it is not known whether a complex collection of maser groups represents a cluster of stars or a cluster of molecular fragments excited by a single star. This is a major problem which must be clarified for a correct interpretation of the maser emission in young star-forming regions.

On the basis of the distributions of sizes and separations discussed in the previous section, we use the term *group* to indicate a collection of maser spots of one species which appear to be closely associated (generally on a scale size <30 mpc). An *isolated* group is one which has no maser of the other species nearer than ~ 150 mpc. A *simple* maser association is composed of one OH and one H_2O group with angular separation less than the positional uncertainty. A *complex* association contains multiple groups of OH and H_2O masers intermixed within an area ~ 150 mpc in extent.

Applying the above definitions we find that in the 74 fields observed with the VLA there are 30 isolated H_2O groups, 16 isolated OH groups, 39 simple and 14 complex associations. There are a further six associations which do not strictly fit into any of these categories, but which we have categorized as isolated. In these six cases the OH and H_2O groups are clearly not coincident, yet they have projected linear separations <150 mpc. The minimum separation between OH and H_2O groups in these associations is typically 80 mpc (4.5″). Although not among the sources in our sample, a good example of this kind of association is the well-known source W3 (OH). If each OH and H_2O group in these associations represents an individual star, their relatively small displacement may indicate that they are members of a cluster or a binary pair.

The total number of sources in each category is given below:

Isolated groups:	22 OH	(4 with H II)
	36 H_2O	(0 with H II)
Simple associations:	39 OH/H_2O	(7 with H II)
Complex associations:	14 OH/H_2O	(9 with H II)

The type of source (or sources) contained in each field observed is listed in Table 1, with uncertain or ambiguous classifications enclosed in parentheses.

Isolated maser groups have spatial and velocity extents similar to groups in close associations. An example is 359.62–0.25 (Fig. 1), which contains an isolated H_2O group with a projected separation from the nearest OH group of ~ 500 mpc. Owing to their isolation, these maser groups are good candidates for excitation by individual stars. The higher proportion of isolated H_2O groups compared to OH groups implies that either H_2O masers have a somewhat longer duration than OH masers, or H_2O masers can additionally occur under conditions unsuitable for OH maser emission, e.g. in the vicinity of lower mass stars. We might then expect that almost all fields containing OH masers should also show H_2O emission.

The pair of OH and H_2O groups nearest the continuum source in Fig. 1 is an example of a simple association. The "simple" classification for this association is uncertain, however, owing to the rather large extent of the H_2O group, and the presence of a nearby H II region. Two other examples of simple associations (with more certain classification) are given in Fig. 7. In most simple associations the OH extent ranges from ~ 5 to 30 mpc with a somewhat smaller extent in H_2O emission. Thus these associations bear a resemblance to evolved stars, which consist of a core of H_2O masers surrounded by a larger shell of OH emission. The diameter of OH shells in evolved supergiants is ~ 30 mpc (Baud, 1981), i.e. about twice the median extent of OH emission in our sample.

The spatial structure of these simple associations is consistent with an embedded star as the exciting source for the maser emission. If a single star is responsible for the maser emission in these sources, the large proportion of simple associations suggests that both molecular species are present during much of the maser phase of star formation.

The 14 associations which we categorize as complex are characterized by the presence of several (3 to 8) OH and H_2O groups spread over typically ~ 150 mpc. The OH and H_2O maser groups generally appear intermixed, although the spatial and velocity distributions are not well correlated in the two species. Complex associations generally have higher maser intensities than simple associations, and broader velocity extents in one or both maser lines. There is little similarity in structure among the complex associations in our sample, although a linear arrangement of maser features appears to be a common feature. Many of the complex associations contain a compact H II region. It is in these complex sources that we are confronted with the difficult question: does each maser group contain an embedded star, or is a single source responsible for all the maser emission? Two examples of complex associations are shown in Fig. 8.

The lifetime of the H_2O maser phase in star forming regions has been estimated at $\sim 10^5$ yr (Genzel and Downes, 1979). If all masers exist within a ~ 30 mpc diameter stellar envelope, a lifetime of $\sim 10^5$ yr is expected for each maser group of this size in both simple and complex associations. On the other hand, if maser emission can also occur in molecular fragments ejected by the star in its later evolutionary stages, complex associations might persist for only a fraction of the total maser phase.

The close association of many maser complexes with a compact H II region confirms the presence of at least one massive star in the complex. However, the irregular distribution of maser groups does not support the notion that the masers form in a spherical shell around the H II region. It may be that the maser groups represent fragments of a shell surrounding the ionized zone, or dense interstellar gas excited by material ejected from the star. Alternatively, it is possible that each maser group contains an embedded star or protostar. Either interpretation could explain the number of compact maser groups found in these associations. If each maser group marks the location of a young star, the maser observations could be used to estimate the density and kinematics of stars in young clusters. This would be extremely useful since little is known about such young clusters because of optical obscuration. On the other hand, if a single star can excite many maser groups over a large distance, the maser

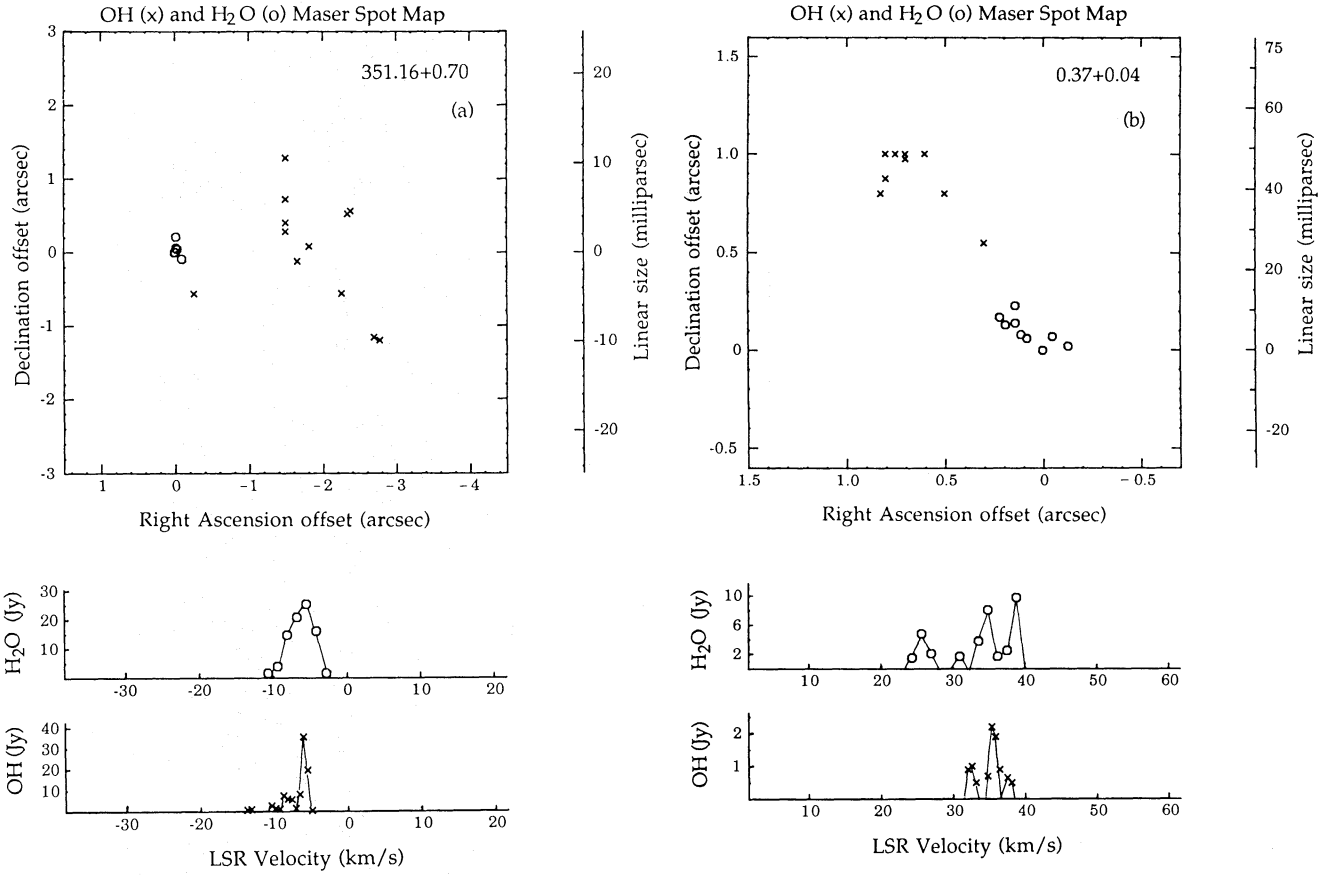

Fig. 7a and b. Spot maps and VLA spectra of the OH (×) and H_2O (○) emission in the fields 351.16+0.70 (reference position $17^h16^m36.08^s$, $-35°54'51.0''$) and 0.37+0.04 (reference position $17^h43^m11.23^s$, $-28°34'34.0''$). These are two examples of simple OH/H_2O maser associations

observations may be used to probe conditions around these stars provided the conditions under which maser action occurs is understood.

If each maser group in a complex association represents a separate star, then the density of stars in these regions amounts to around 3 to 8 stars in an area ~150 mpc in diameter. Such star densities are observed in active regions such as Orion, and have been inferred from radio continuum observations for a few of the fields in our sample (Ho and Haschick, 1981). The association of each maser group with an individual star in a dense cluster would account for the intermixing of OH and H_2O maser groups in complex associations; it would also account for the compact size of the groups, the wide velocity spread within a group, and provide a source of excitation for each group. In this interpretation maser emission arises in a dense molecular envelope with a diameter <30 mpc. OH and H_2O molecules in the envelope are pumped by an embedded stellar source, much as in evolved stars. Early VLBI observations of H_2O masers were interpreted in this way (Genzel et al., 1978). Combined OH, H_2O and continuum observations towards Cepheus A (Cohen et al., 1984) also provides evidence of maser emission associated with several individual stars in a compact cluster.

The embedded star model encounters difficulties however, when applied to the complex associations in our sample. If each maser group in a complex association contains an embedded star, then each OH group should be nearly coincident with an H_2O group as in simple associations. This would produce a good correlation between OH and H_2O groups, as observed in Cepheus A. However, a close correlation is not generally observed for the complex associations in our sample. Another problem is related to the expected lifetime of $\sim 10^5$ yr for the maser phase, and the size of the associated H II region when present. If we assume that the compact H II regions in these associations have expansion velocities $\sim 5\ km\ s^{-1}$, then maser emission should be present until the H II region reaches a diameter of ~1000 mpc if the OH and H_2O masers endure for $\sim 10^5$ yr. However, Habing et al. (1974) have shown that OH maser emission is not found near H II regions whose diameters exceed ~100 mpc. The results of this study, along with the high detection rate of H_2O maser emission at the locations of OH masers in the galaxy (Caswell et al., 1983a, b), suggests that this result also applies for H_2O masers. We therefore conclude that the OH and H_2O maser emission in complex associations persists for a time short compared to 10^5 yr, then disappears.

We suggest that isolated maser groups and simple OH/H_2O associations are excited by a single embedded star. Simple associations last for nearly 10^5 yr, and correspond to the accretion phase of massive star formation. In this phase the ionized region is kept small by accretion of molecular material, and maser emission is confined to a diameter <30 mpc. We further suggest that complex maser associations evolve from these simple associations, and correspond to an expansion phase of massive star

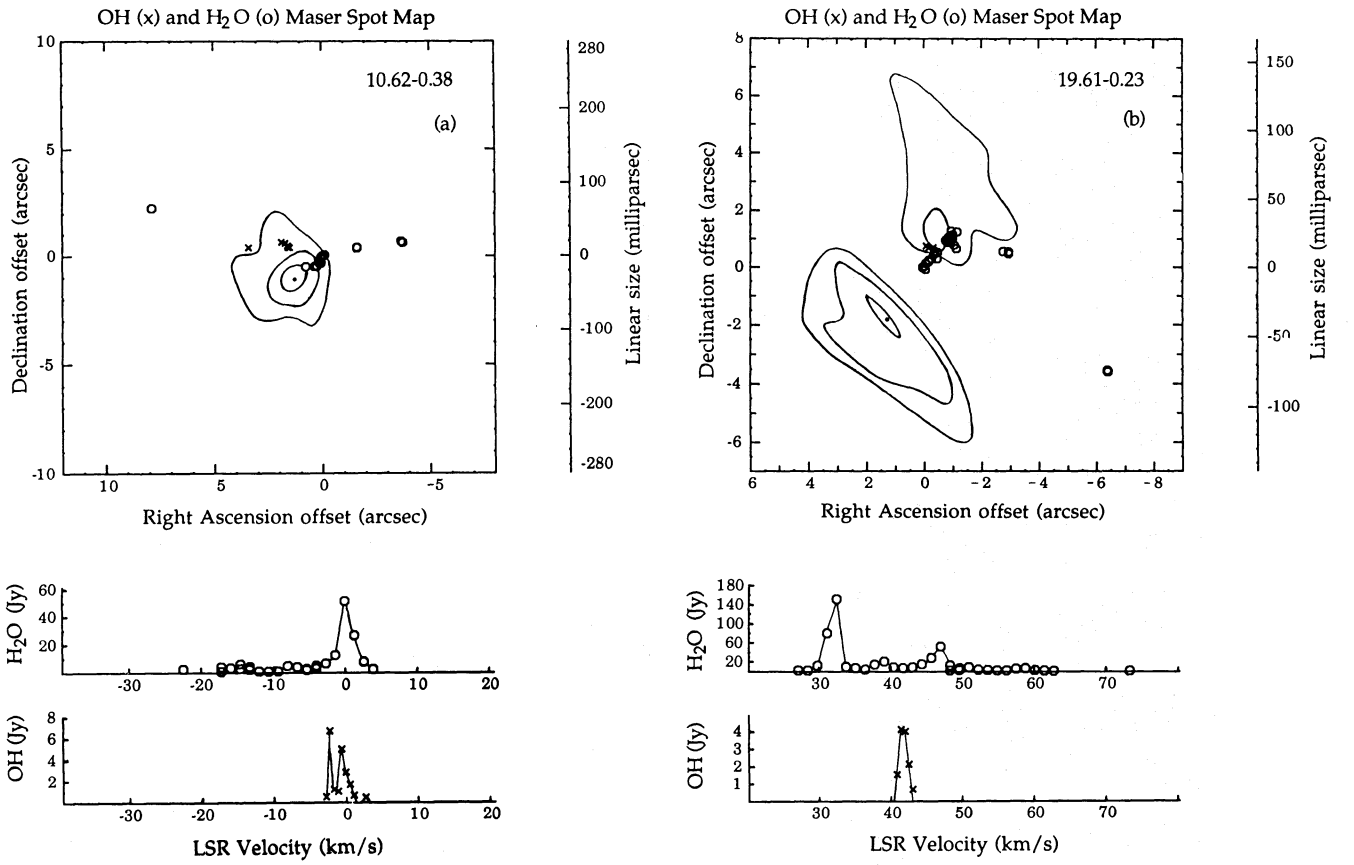

Fig. 8a and b. Spot maps and VLA spectra of the OH (×) and H_2O (○) emission in the fields 10.62−0.38 (reference position $18^h07^m30.56^s$, $-19°56'28.8''$) and 19.61−0.23 (reference position $18^h24^m50.25^s$, $-11°58'31.7''$). These are two examples of complex OH/H_2O associations containing compact H II regions. Contours of the 22 GHz continuum emission are shown at levels of 55, 220 and 440 mJy/beam for 10.62−0.38, and at 80, 165 and 310 mJy/beam for 19.61−0.23

formation. The individual maser groups in these associations do not contain embedded stars; they occur in small molecular fragments excited by outflow from a central massive star. These masers represent an energetic, short-lived and final stage in the total maser phase. Our preference for this interpretation is based on a comparison of OH and H_2O maser groups in simple and complex associations, and on the frequent occurrence of H II regions in the complex sources. In addition, the proper motion studies of Genzel et al. (1981) and others give compelling evidence for the existence of small masing fragments which are unlikely to contain embedded stars.

We will henceforth refer to this as the "molecular fragment" model, in contrast to the "embedded star" model in which each maser group contains an internal source of excitation. In the molecular fragment model, maser excitation comes from a nearby star or H II region in the form of radiation and kinetic energy. While direct radiative pumping from a non-embedded source can be ruled out in some cases (Forster et al., 1977), indirect processes involving collisions (Tarter and Welch, 1986) and more distributed FIR fields are viable radiative pumping mechanisms.. Mass outflow from the star provides a mechanism for collisional pumping over large distances, especially if the flow is highly collimated. The masing molecular fragments may be material ejected from the star, material still bound to the star, or nearby ambient material unrelated to the formation of the exciting star. Linear features are accommodated in this model by invoking collimated outflow, or by excitation of existing linear structures such as discs viewed edge-on, or the boundaries of dense clouds. In the following section our general picture of maser emission in star forming regions is described in more detail.

5. Interpretation

We begin our discussion with a brief review of the observed and inferred properties of OH and H_2O masers. Unfortunately, only broad limits on the density and temperature of interstellar masers are available from theoretical considerations, and no pumping mechanism has yet become generally accepted. A typical OH maser has a spot size of ~0.1 mpc, a density in the range 10^7 to 10^8 cm^{-3}, and a temperature around 100 K. The timescale for substantial variations in OH maser intensity and velocity is on the order of months to years. The velocity spread within an OH group is typically ~6 km s^{-1}, and magnetic field strengths inferred from Zeeman splitting are a few milligauss. H_2O masers have a wider velocity spread (10 to 100 km s^{-1}) smaller spot size (0.01 mpc), and higher densities (10^8 to 10^9 cm^{-3}) and temperatures than OH masers. H_2O maser emission varies on timescales from days to months, sometimes flaring briefly or disappearing

for periods of time. Because of a low g-factor, Zeeman splitting cannot provide an estimate of the magnetic field strength in H_2O masers.

The general conditions required for maser emission are present in warm, dense environments, such as the molecular envelopes surrounding young stars in the accretion phase. Inside these dense cocoons enough energy is available to pump most maser sources, and a diameter <30 mpc is theoretically inferred for these objects (e.g. Yorke and Krugel, 1977). We have shown in the previous section that simple OH/H_2O maser associations have a structure consistent with maser formation in such young stellar envelopes, and argued that complex associations may represent a later evolutionary stage of these stars. Using current theoretical models along with the observed spatial structure of maser regions from this study and others, an evolutionary sequence for the formation of OH and H_2O masers in star-forming regions is outlined below.

Isolated H_2O groups probably represent the youngest phase of star formation in which maser emission is present. The appearance of a compact H_2O group may mark the commencement of nuclear burning in the core of an accreting protostellar object. As nuclear burning and accretion continue, the dusty molecular envelope surrounding the core warms up and OH emission soon accompanies the H_2O emission. The OH masers arise in more extended, lower density regions at greater distances from the protostellar core than the H_2O masers. The material from which the OH and H_2O masers form is in accretion at this stage, and the pump may be radiative or collisional, or a combination of both.

The structural and kinematical evolution of massive pre-main sequence stars has recently been treated by Kolesnik and Kravchuk (1983). They postulate a non-steady accretion of material at the dust-melting radius (r_m) via successive build up and disruption of dusty cocoons. The simple OH/H_2O maser associations may represent stars in a quasi-equilibrium accretion stage similar to this. The H_2O masers are located in the dense inner parts of the cocoon, and OH masers farther out in the accreting envelope. Since simple associations make up the majority of our sample, this is the longest phase during which both OH and H_2O masers are present.

For a core mass of 10 $M_\odot$, accretion velocities range from $\sim 5\,\mathrm{km\,s^{-1}}$ at a few mpc to $\sim 20\,\mathrm{km\,s^{-1}}$ at the dust-melting radius (<0.1 mpc). Inside r_m an H II region forms whose diameter slowly expands with increasing stellar luminosity. The ionization front advances slowly during the accretion phase, because neutral material is continually available to absorb the increasing number of ionizing photons. The intensity of 22 GHz radio emission from the ionized gas is <100 mJy until the H II region reaches a diameter of $\sim 0.2''$ (5 mpc at a distance of 5 kpc). H_2O masers form nearer the core, and therefore have wider velocity extents and are more compact than OH groups. The accreting material will not be spherically distributed if angular momentum or magnetic fields are important, and repeated fragmentation of the supporting dust cocoon will produce spotty and irregular maser groupings spread over a few mpc.

As the stellar luminosity increases r_m moves farther out where the accretion velocity is lower, and eventually a balance between gravity and radiation pressure is reached. Formation and disruption of successive cocoons continues, but, according to Kolesnik and Kravchuk (1983), when the retarding velocity due to radiation pressure exceeds the free-fall velocity the fragments are driven away rather than falling onto the star. At this point the OH maser emission has reached a diameter of ~ 30 mpc and the flow of neutral material through the dust cocoon stops. As internal pressures continue to increase, dense clumps are ejected from the star and the molecular envelope is dispersed into the interstellar medium.

A complex maser association is the end-product of this dispersion, the earliest phase of which is a simple maser association with large H_2O velocity spread. The H_2O emitting gas closest to the star experiences the greatest acceleration, and is ejected into the more distant OH emitting regions in compact clumps. Since neutral material is no longer being accreted inside r_m, the H II region begins to expand. The expanding H II region, along with radiation pressure and stellar winds, soon causes the more distant OH emitting region to break up and move away from the star. This is in contradiction to the model of Reid et al. (1980), who proposed that OH masers associated with well-developed H II regions form in material which is still being accreted. In addition to the ejected H_2O masers, outflow from the star excites more maser emission in the surrounding interstellar gas (Tarter and Welch, 1986). This emission occurs at the velocity of the ambient material, while high-velocity emission from the ejected fragments may also be present. These masers show up in dense molecular gas located within ~ 150 mpc of the star, particularly in directions of greatest mass outflow. The expansion phase is the final stage of maser emission; as the region expands and the material near the star is dispersed, the masers disappear.

The small number of complex maser groups in our sample implies that the expansion phase is short compared with the total maser phase of star formation. The size-velocity diagrams discussed in Sect. 3.5 may be used to obtain an estimate of the duration of this phase. The spatial extent of OH maser emission is apparently bounded by an upper limit proportional to the velocity extent, corresponding to $\sim 10\,\mathrm{mpc/km\,s^{-1}}$. Although less apparent, a similar limit may also hold for H_2O masers. In a free-expansion model this limit corresponds to a maximum expansion time of 10^4 years for an ensemble of sources with different expansion velocities. The physical significance of this limit may be related to the maser pump mechanism. For example, if pump energy is acquired via collisions with material whose density falls rapidly with distance from the star, the maser lifetimes may be similar for a broad range of ejection velocities. This might explain the size-velocity correlation observed for OH masers in the expansion phase. The lack of a strong correlation for H_2O masers may indicate that a different pumping mechanism applies for them. Since $\sim 10\%$ of the maser sources observed in this study are complex, our estimate for the total duration of the maser phase is $\sim 10^5$ years, in agreement with Genzel and Downes (1979).

Many of the observed properties of OH/H_2O maser associations can be accounted for in this scenario. It is a synthesis of current ideas on star formation, now guided by observational data for a large number of maser sources. The evolutionary sequence proposed here is based mainly on the OH/H_2O associations in our sample, yet it is similar to the scheme proposed by Genzel and Downes (1977) which was based on the appearance of H_2O maser spectra. New observations and a better theoretical understanding will undoubtedly improve further our picture of the maser phenomenon in star-forming regions. High resolution observations of molecular line transitions with critical densities between 10^4 and $10^7\,\mathrm{cm^{-3}}$ would be of particular value.

6. Conclusion

VLA observations of ~70 OH/H_2O masers associated with star-forming regions show that the two molecular species generally occur close together and in compact groups less than ~30 mpc in diameter. H_2O groups are usually smaller, more numerous and have a wider velocity spread than OH groups. In complex associations containing H II regions and many maser groups, the H_2O groups are often spread over a larger area than OH groups and typically cluster on a scale of ~150 mpc, comparable with the size of the H II region. In these associations OH and H_2O groups are spatially intermixed, but usually not coincident.

We have shown that complex OH/H_2O maser associations may be interpreted either as a dense cluster of young stars, or as a collection of masing molecular clumps associated with a single star. We have argued that the latter is probably the case for the complex associations in our sample. However, the former interpretation may be the correct one in a few instances, and in such cases the masers provide a useful window into the structure and kinematics of young star clusters.

We have given a scenario for star formation which places various types of maser associations in an evolutionary sequence. We suggest that isolated H_2O masers appear first, and form near the cores of massive protostars at the commencement of nuclear burning. They are soon followed by OH emission which forms in less dense circumstellar material surrounding the core. These simple OH/H_2O associations last about 10^5 years and correspond to an accretion phase during which the OH region reaches a diameter of ~30 mpc. Accretion terminates when internal pressures reverse the flow of neutral material, causing fragments of dense molecular material to be thrown out as H_2O masers, and causing the OH emitting region to break up and move away from a rapidly developing H II region. The resulting complex association of OH and H_2O maser groups expands to ~150 mpc over the next 10^4 years, then disappears.

In a forthcoming paper, we will analyse some of the individual regions in detail and attempt to assign each to its appropriate place in the general evolutionary sequence given above.

Acknowledgements. We are grateful to the VLA staff; without their generous aid the completion of such an ambitious project would have been impossible. We are especially indebted to Jacqueline van Gorkom, whose presence in several moments of crisis saved us from disaster. We thank Bill McCutcheon for useful discussions, and gratefully acknowledge the help of J.R. Price, who performed much of the detailed analysis of the OH maps while JLC was visiting the Dominion Radio Astrophysical Observatory (DRAO). JLC gratefully acknowledges the kind hospitality and assistance of the DRAO staff, and travel support from DRAO for this project.

References

Baart, E.E., Cohen, R.J.: 1985, *Monthly Notices Roy. Astron. Soc.* **213**, 641

Baud, B.: 1981, *Astrophys. J.* **250**, L79

Baudry, A., Forster, J.R., Welch, W.J.: 1974, *Astron. Astrophys.* **36**, 217

Brebner, G.C., Heaton, B., Cohen, R.J., Davies, S.R.: 1987, *Monthly Notices Roy. Astron. Soc.* **229**, 679

Caswell, J.L., Haynes, R.F.: 1983a, *Australian. J. Phys.* **36**, 361

Caswell, J.L., Haynes, R.F.: 1983b, *Australian. J. Phys.* **36**, 417

Caswell, J.L., Batchelor, R.A., Forster, J.R., Wellington, K.J.: 1983a, *Australian. J. Phys.* **36**, 401

Caswell, J.L., Batchelor, R.A., Forster, J.R., Wellington, K.J.: 1983b, *Australian. J. Phys.* **36**, 443

Cheung, A.C., Rank, D.M., Townes, C.H., Thornton, D.D., Welch, W.J.: 1969, *Nature* **221**, 626

Cohen, R.J., Rowland, P.R., Blair, M.M.: 1984, *Monthly Notices Roy. Astron. Soc.* **201**, 425

Cook, A.H.: 1968, *Monthly Notices Roy. Astron. Soc.* **140**, 299

Deguchi, S.: 1981, *Astrophys. J.* **249**, 145

Elitzur, M., de Jong, T.: 1978, *Astron. Astrophys.* **67**, 323

Forster, J.R., Welch, W.J., Wright, M.C.H.: 1977, *Astrophys. J. Letters* **215**, L121

Forster, J.R., Welch, W.J., Wright, M.C.H., Baudry, A.: 1978, *Astrophys. J.* **221**, 137

Freund, J.E.: 1971, *Mathematical Statistics*, Prentice Hall, New Jersey

Garay, G., Reid, M.J., Moran, J.M.: 1985, *Astrophys. J.* **289**, 681

Gaume, R.A., Mutel, R.L.: 1987, *Astrophys. J. Suppl.* **65**, 193

Genzel, R., Downes, D.: 1977, *Astron. Astrophys. Suppl.* **30**, 145

Genzel, R., Downes, D.: 1979, *Astron. Astrophys.* **72**, 234

Genzel, R., Downes, D., Moran, J.M., Johnston, K.J., Spencer, J.H., Walker, R.C., Haschick, A.D., Matveyenko, L.I., Kogan, K.R., Kostenko, V.I., Ronnang, B., Rydbeck, O.E.H., Moiseev, I.G.: 1978, *Astron. Astrophys.* **66**, 13

Genzel, R., Reid, M.J., Moran, J.M., Downes, D.: 1981, *Astrophys. J.* **244**, 844

Habing, H.J., Goss, W.M., Matthews, H.E., Winnberg, A.: 1974, *Astron. Astrophys.* **35**, 1

Heaton, B.D., Matthews, N., Little, L.T., Dent, W.R.F.: 1985, *Monthly Notices Roy. Astron. Soc.* **217**, 485

Hills, R., Janssen, M.A., Thornton, D.D., Welch, W.J.: 1972, *Astrophys. J.* **175**, L59

Ho, P.T.P., Haschick, A.D.: 1981, *Astrophys. J.* **248**, 622

Kolesnik, I.G., Kravchuk, S.G.: 1983, *Soviet Astron.* **27**, 513

Mader, G.L., Johnston, K.J., Moran, J.M.: 1978, *Astrophys. J.* **224**, 115

Mezger, P.G., Robinson, B.J.: 1968, *Nature* **220**, 1107

Norman, C., Silk, J.: 1979, *Astrophys. J.* **228**, 197

Norris, R.P.: 1984, *Monthly Notices Roy. Astron. Soc.* **207**, 127

Reid, M.J., Haschick, A.D., Burke, B.F., Moran, J.M., Johnston, K.J., Swenson, G.W.: 1980, *Astrophys. J.* **239**, 89

Tarter, J.C., Welch, W.J.: 1986, *Astrophys. J.* **305**, 467

Weaver, H., Williams, D.R.W., Dieter, N.H., Lum, W.T.: 1965, *Nature*, **208**, 29

Yorke, H.W., Krugel, E.: 1977, *Astron. Astrophys.* **54**, 183